Neurochemical Research (2019) 44:1533–1548
https://doi.org/10.1007/s11064-019-02774-9

ORIGINAL PAPER

Iron Oxide Nanoparticles Affects Behaviour and Monoamine Levels in Mice

Vijayprakash Manickam[1] · Vasanth Dhakshinamoorthy[1] · Ekambaram Perumal[1]

Received: 29 August 2018 / Revised: 8 March 2019 / Accepted: 9 March 2019 / Published online: 2 April 2019

Abstract

Iron oxide (Fe_2O_3) nanoparticles (NPs) attract the attention of clinicians for its unique magnetic and paramagnetic properties, which are exclusively used in neurodiagnostics and therapeutics among the other biomedical applications. Despite numerous research findings has already proved neurotoxicity of Fe_2O_3-NPs, factors affecting neurobehaviour has not been elucidated. In this study, mice were exposed to Fe_2O_3-NPs (25 and 50 mg/kg body weight) by oral intubation daily for 30 days. It was observed that Fe_2O_3-NPs remarkably impair motor coordination and memory. In the treated brain regions, mitochondrial damage, depleted energy level and decreased ATPase (Mg^{2+}, Ca^{2+} and Na^+/K^+) activities were observed. Disturbed ion homeostasis and axonal demyelination in the treated brain regions contributes to poor motor coordination. Increased intracellular calcium ($[Ca^{2+}]_i$) and decreased expression of growth associated protein 43 (GAP43) impairs vesicular exocytosis could result in insufficient signal between neurons. In addition, levels of dopamine (DA), norepinephrine (NE) and epinephrine (EP) were found to be altered in the subjected brain regions in correspondence to the expression of monoamine oxidases (MAO). Along with all these factors, over expression of glial fibrillary acidic protein (GFAP) confirms the neuronal damage, suggesting the evidences for behavioural changes.

Keywords Brain markers · Demyelination · Energy depletion · Fe_2O_3-NPs · Monoamines · Neurobehaviour

Introduction

Among the engineered nanoparticles (NPs), iron oxide (Fe_2O_3) NPs are the most favourable choice in industrial and biomedical applications, since it is noted for magnetic properties, low cost and high resistance to corrosion [1]. Applications of Fe_2O_3-NPs in clinical diagnostics and therapeutics are growing remarkably [2] including magnetic resonance imaging (MRI) of gastrointestinal tract [3–5], brain [6] and targeted drug delivery [7]. Simultaneously, potential neurotoxicity of Fe_2O_3-NPs has also been on rise along with its applications. The deleterious impact of iron toxicity due to the repeated exposure and bioaccumulation are of a serious concern. Biomedical applications of Fe_2O_3-NPs have been shown to be the source of iron accumulation in biological systems regardless of the routes of administration [8]. Though the brain is tightly protected by blood–brain barrier, Fe_2O_3-NPs potentially traverse and accumulate in the brain regions, which make the Fe_2O_3-NPs more promising in neuroimaging [9]. As contrast agent, a mass of more than 200 mg of Fe_2O_3 NPs is injected to human in MRI [10]. The translocation of Fe_2O_3-NPs into central nervous system (CNS) increases the brain vulnerability to free radical toxicity [11]. Exposure to Fe_2O_3-NPs has been reported to cause oxidative stress, neurodegeneration [9, 12, 13], neuronal apoptosis [8] and neurobehavioural impairments in animal models [14–16]. Further, oral administration of Fe_2O_3-NPs seems to cause defective synaptic transmission and nerve conduction in rats [17]. Thus, deeper understanding of Fe_2O_3-NPs mediated neurotoxicity is crucial to design safer therapeutic applications.

Electronic supplementary material The online version of this article (https://doi.org/10.1007/s11064-019-02774-9) contains supplementary material, which is available to authorized users.

Vijayprakash Manickam and Vasanth Dhakshinamoorthy have equally contributed to this research work.

✉ Ekambaram Perumal
ekas2009@buc.edu.in

[1] Molecular Toxicology Laboratory, Department of Biotechnology, Bharathiar University, Coimbatore, Tamil Nadu 641 046, India

The release of monoamines into synopsis are pivotal in mediating the neuronal processes underlying behaviour [18]. Motor control and sensory processing is governed by dopamine [19] and norepinephrine [20] respectively which orchestrates the optimization of behaviour. Studies have shown that the altered levels of monoamine underlie the root cause for behavioural changes. However, studies emphasizing impacts of Fe_2O_3-NPs on behaviour and monoamine levels are limited.

Although the neurotoxic impacts of Fe_2O_3-NPs is proven, the key factors responsible for the behavioural impairments remain ambiguous. Thus, a focus on the components of neuronal conduction upon Fe_2O_3-NPs exposure would help to understand neurotoxicity in the context of animal behaviour to further extent. Since the neuronal ion concentration [17], energy homeostasis [21], myelination of axons and proper vesicular exocytosis are important for the release of catecholamines such as dopamine (DA), norepinephrine (NE) and epinephrine (EP). In the current study, we have investigated the status of mitochondrial damage, energy level, degree of demyelination, machinery of vesicular exocytosis and monoamine metabolism upon repeated oral exposure to Fe_2O_3-NPs.

Materials and Methods

Nanoparticles Preparation

Fe_2O_3-NPs powder was purchased from Sigma Aldrich (catalog # 544884) and characterized. 25 mg of NPs was dispersed in 1 ml of 0.9% saline, ultra-sonicated at 20 Hz for 20 min at 4 °C. The NPs were freshly prepared for each administration.

Animals and Experimental Design

Eight weeks old male Albino mice (*Mus musculus*) weighing 25 to 30 g were purchased from Experimental Animal Centre (Kerala Agricultural University, Trissur, India), 3 animals were housed per cage and maintained under standard laboratory conditions. The experiments were conducted in accordance with the ethical norms approved by Institutional Animal Ethical Committee (722/02/A/CPCSEA). The animals were randomly divided into three groups (n = 5 per group). Test groups were orally (i.e. gavage) administered with 25 and 50 mg of Fe_2O_3-NPs/kg bw once a day for 30 consecutive days and control group received same volume of 0.9% saline for the same duration. Different set of animals were used for each behavioural analysis, biochemical assays and molecular experiments. The doses were chosen based on exposure range of Fe_2O_3-NPs in oral biomedical applications [22] and our earlier studies [8, 23]. Neurotoxicity has been observed in rats orally exposed with 100-1000 mg/kg/day of Fe_2O_3-NPs for 28 days [17], however we have examined in lower doses. After 24 h of the last treatment, animals were sacrificed by cervical decapitation, blood was collected and serum was separated. The brain was isolated intact; washed with 0.9% saline and the brain sub regions viz., frontal cortex, cerebellum and hippocampus were chosen for the analysis as the former is responsible for motor coordination and the later for learning and memory. The brain sub regions were carefully dissected and used for analyses.

Behavioural Studies

Behaviour of animals were analysed to understand the impact of Fe_2O_3-NPs on motor-coordination and learning and memory.

Spontaneous motor activity (SMA) was assessed using an activity monitoring apparatus [24]. The sensors implanted at the floor of the apparatus were sensitive to the vibrations of the animals and measures all the activities (locomotion, scratching and grooming). The activity of each animal inside the chamber was measured for 10 min. The SMA was expressed as counts/10 min.

Motor coordination of animals was analysed using rotarod apparatus [25]. The animals were forced to stay on the rough surface of the horizontal rod (5 cm diameter; 30 cm long) rotating at 14 rpm on its axis. The animals having defective motor function cannot withstand and would fall off from the rotating rod. Each animal was allowed a test period of 90 S. The endurance time (S) was calculating as the time between placing the animal on the rotating rod, and the moment animal fell down, which was automatically recorded by the software SMART V3.0.03.

Footprint analysis was performed to evaluate gait pattern of control and test animals [26]. Animals were placed in a 10 cm wide and 100 cm long runway floor which was covered with white absorbance paper. Before the NPs exposure, the animals were trained to pass straight forward through the corridor. After training, animals were treated with Fe_2O_3-NPs, the paws were stained (fore-paws with green and the hind-paws with red) and animals were allowed to walk down the corridor. Sway length, stance length, stride length and inter-limb distances were measured.

Morris water maze experiment was performed to assess the effect of Fe_2O_3-NPs on learning and spatial memory [16, 27]. The water maze apparatus, a circular pool, (160 cm diameter; 60 cm depth; Panlab Harvard Apparatus), was filled with water to the depth of 50 cm and the temperature of water was maintained at 24 ± 1 °C. A resting platform (10 cm diameter) was submerged (1 cm) at the centre of the pool for the learning trials, and for the memory probe test, water was made opaque in order to rule out visual cue. Movement of the animals were tracked using SMART

V3.0.03 software. The latency (time required to find the platform) was measured in control and NPs treated animals and expressed in S.

Elemental Analysis

The elemental analysis was done by the protocol described by Wang et al. [9]. Inductively coupled plasma mass spectrometry (IC-MS) was used to measure the concentration of Mg^{2+}, Na^{+}, K^{+} and Fe^{2+} in serum (µg/dl) and brain regions -frontal cortex, hippocampus and cerebellum (µg/g wet tissue).

Mitochondrial Analysis

Mitochondria were isolated from the brain regions as per Qiagen protocol (catalog # 37612). The mitochondria with undamaged outer membrane were estimated as described in the product information by Sigma Aldrich (catalog # CYTOCOX1).

ATP Determination

Tissues of brain regions were individually homogenized with ice cold lysis buffer (25 mM Tris, pH 7.5, 4 mM EGTA, 1% Triton X-100, 10% glycerol, 2 mM dithiothreitol). ATP levels in the brain regions was analysed by firefly luciferase-based ATP detection kit as per manufacturers' protocol (Thermo Fisher Scientific, Texas, USA).

Western Blotting

Expression pattern of neuronal dysfunction and cell death markers were analyzed in the frontal cortex, hippocampus and cerebellum of control and treated animals. To analyze the mitochondrial damages, the mitochondria and cytoplasm were separated as described by Qiagen protocol (catalog # 37612). Blotting was performed by the standard protocol as described [16]. Membranes with the mitochondrial and cytoplasmic lysate fractions were incubated overnight with primary antibodies of mouse anti-cytochrome c (1:2000). The membranes with whole cell lysate were incubated with mouse anti-cytochrome c (1:2000) and mouse anti-heat shock protein 27 (HSP27) (1:2500). Glyceraldehyde-3-phophate dehydrogenase (GAPDH) and Cytochrome c oxidase IV (Cox IV) were used as loading controls for cytoplasmic and mitochondrial fractions respectively.

To examine the glial fibrillary acidic protein (GFAP) and vesicular exocytosis aiding protein (growth associated protein 43, GAP43) expression, the brain regions were homogenized with ice-cold RIPA buffer. The homogenate was centrifuged at 12000 rpm for 20 min at 4 °C and the supernatant was collected. The protein was estimated by Bradford method. Protein lysates were loaded in 10% SDS PAGE gel and transferred, blocked with 5% fat free skim milk and incubated individually with rabbit anti-GFAP (1:5000), rabbit anti-GAP43 (1:5000) and mouse anti-GAPDH.

The proteins were detected using horseradish peroxidase (HRP)-conjugated anti-rabbit, anti-goat or anti-mouse secondary antibodies (1:2500) and visualized by DAB staining (0.02% DAB in 0.01% H_2O_2). The same procedure was followed for hippocampus and cerebellum lysates. GAPDH was used as the internal control to ensure equal sample loading and Western transfer. Densitometry analyses of immunoblots were quantified using *ImageJ* analysis software from National Institute of Health (NIH).

Estimation of ATPase

Ca^{2+}, Mg^{2+} and Na^{+}/K^{+} ATPase activities were measured using spectrophotometer by the method described by Hjerten and Pan [28], Ohnishi et al. [29] and Bonting et al. [30] respectively.

Lipid Peroxidation

Lipid peroxidation (LPO) produce malondialdehyde (MDA), which reacts with thiobarbituric acid (TBA) to form a pink chromogen. MDA and TBA adduct was estimated by its absorbance at 532 nm and expressed as nM/mg protein [31].

TEM Analysis

After the treatment period, animals were subjected to vascular perfusion with the mixture of 2.5% glutaraldehyde and 2% paraformaldehyde, made in 0.1 M sodium phosphate buffer (pH 7.4). The brain regions were fixed with the same fixative at 4 °C. After fixation about 2 mm of respective brain regions were excised and further trimmed into 1 mm pieces. The tissues were osmicated, dehydrated and embedded in araldite CY212. The area from 500 nm block was selected using light microscope after staining with 0.5% toluidine blue. The blocks were cut by using ultramicrotome contrasted with uranyl acetate and lead citrate and observed under TECANI G20 transmission electron microscope (FEI Company, Netherland).

High Performance Liquid Chromatography (HPLC)

The frontal cortex, hippocampus and cerebellum of the control and experimental animals were dissected and homogenized with 0.1 M trichloroacetic acid, 10 mM sodium acetate and 0.1 mM EDTA (pH 3.75). 1% isoproterenol was used as internal control. The supernatant was filtered through 0.2 µ filter and 20 µl of filtrate was injected into HPLC. Standard stocks of DA, NE and EP were made at a concentration of

1 mg/ml and serially diluted to obtain a concentration of 10 pg/µl of injection volume. The analysis was done using isocratic ion-pair HPLC (Shimadzu Co., Kyoto, Japan) with electrochemical detection (Biorad, Richmond, CA, USA). The HPLC analysis was performed as described by Kim et al. [32] and Chen et al. [33].

Immunohistochemistry (IHC)

Frontal cortex (motor region), hippocampus (CA1) and cerebellum (arbour vitae and cerebellar cortex) tissue sections (5 µ) were dehydrated with different graded ethanol solutions. IHC was performed by the standard protocol as previously described [16]. After blocking, the sections were incubated overnight at 4 °C with primary antibody of rabbit anti-GFAP (1:250) and rabbit anti-GAP43 (1:500). Immunoreactions were labelled using a DAB staining kit. Sections were counterstained using haematoxylin and mounted with distrene plasticizer xylene (DPX). Totally five sections (one per animal) were quantified in a blind fashion for depicting the total number of positively stained cells.

Intracellular Calcium ($[Ca^{2+}]_i$) Estimation

The $[Ca^{2+}]_i$ was estimated in the primary cells as described earlier [34]. The fluorescence intensity was also measured at an excitation wavelength of 340 and 380 nm alternately using fluorescence spectrometer (KontronSFM25, Poway, California, USA). Absolute values of $[Ca^{2+}]_i$ was determined based upon the calibration curve [35]. Serum calcium level was estimated using calcium test kit (Arsenazo III) method as described by the manufacturer and expressed as mg/dl.

Measurement of Monoamine Oxidase (MAO) Activity

Mitochondrial fractions of brain regions were isolated immediately after the animal dissection using Qiagen protocol (catalog # 37612). Briefly, isolated mitochondrial fractions were washed with 10 volumes of sodium phosphate buffer and centrifuged at 15000 g for 30 min at 4 °C. The pellet was again suspended with the same buffer. Protein concentration was estimated by Bradford method. MAO-A and B activities were recorded spectrophotometrically as described by [36]. MAO activity was expressed in nM/20 min/mg protein.

Semi-Quantitative RT-PCR

The total RNA was extracted with the RNA purification kit (Fermentas, Waltham, Massachusetts, USA). The first strand cDNA was synthesized from 1 µg of total RNA using first strand cDNA synthesis kit. An aliquot of the first strand cDNA strand was used as a template. Tyrosine hydroxylase (*Th*), *MAO-A* and *MAO-B* primers were as follows: *Th* (F: 5′ATGGAAATGCTGTTCTCAAC3′ and R: 5′GTCTCTAAGTGGTGGATTTTG3′), *MAO-A* (F: 5′CCAAGATCCACTTTAAACCAG3′ and R: 5′AGC CACAATAGTCCTTTTTC3′) and *MAO-B* (F: 5′AGG AAAAAGGATTTCTGTGG3′ and R: 5′CTGGTTTGG TATCATCCAATG3′). The amplification products were electrophoresed on 2% agarose gels to confirm amplification specificity. Relative quantification of gene expression among each sample was achieved by normalization against *β-Actin* (F: 5′TTCTGGAGATACGGTTGTG3′ and R: 5′ TGATCTTCATGGTGCTAGG3′).

Statistical Analysis

All the values were expressed as mean ± SD of five animals in each group. The data were analysed with one-way analysis of variance (ANOVA) followed by Tukey's multiple comparison test using SPSS (20.0) software package. $p < 0.05$ was considered to indicate statistical significance.

Results

Characterization of NPs

The average size of the commercially availed Fe_2O_3-NPs was found to be 45 nm with spherical shape. Also the NPs were found to be pure in maghemite phase. The NPs reveals a net positive charge in suspension with high stability (Supplementary Material, Figs. 1–5).

Exposure to Fe_2O_3-NPs Impairs Behaviour

There was a significant reduction in SMA and rota-rod endurance time in the Fe_2O_3-NPs treated groups in a dose dependent manner (Fig. 1). Footprint analysis shows alteration in paw overlapping patterns. There was an increase in inter-limb distance resulting in the alteration of front-limb and hind-limb coordination ultimately leading to irregular footprint overlapping. Alterations in sway length, stride and stance length were also observed in Fe_2O_3-NPs treated groups (Fig. 2). Morris water maze experiment reveals that the Fe_2O_3-NPs treated animals swim longer to find the hidden platform compared to control. 50 mg/kg treated animals could not able to reach the platform even after 60 S (the maximum latency) whereas; control and 25 mg/kg treated animals reached the platform 6 and 20 S respectively (Fig. 3). This result confirms the occurrence of memory defects in higher dose besides locomotor impairment.

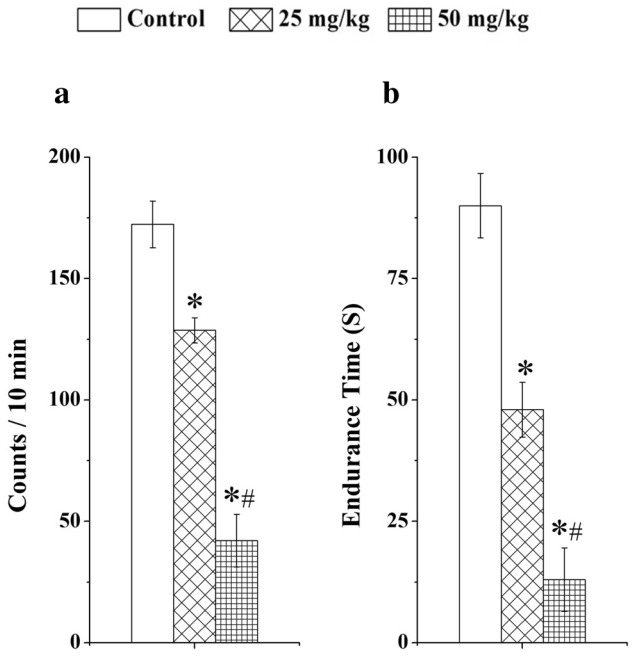

Fig. 1 Exposure to Fe_2O_3-NPs affects locomotor behaviour in mice. **a** Spontaneous motor activity and **b** motor coordination. Values are mean ± SD of five animals. *p < 0.05 compared to control animals; #p < 0.05 compared to 25 mg/kg treated animals (one-way ANOVA followed by Tukey's multiple comparison test)

Bioaccumulation of Iron in Brain

ICP-MS analysis shows the bioaccumulation of iron in the brain regions of NPs treated animals. There was a significant increase in the iron level in Fe_2O_3-NPs treated group compared to control (Table 1). MRI of brain and Prussian blue staining also confirms the iron accumulation in the treated brain regions (Supplementary Material, Figs. 6, 7).

Fe_2O_3-NPs Damages Mitochondria and Depletes Energy Level

There was a significant reduction in the number of mitochondria with undamaged outer membrane in the treated brain regions compared to control. Western blotting analysis of mitochondrial and cytoplasmic lysates shows reduced mitochondrial cytochrome c and increased cytoplasmic cytochrome c. Level of HSP27 was decreased in the brain regions of treated animals. The ultra-structural imaging also confirms remarkable mitochondrial damages in the brain regions of test animals. Luciferase assay shows significant reduction of ATP level in the brain regions of these animals (Fig. 4).

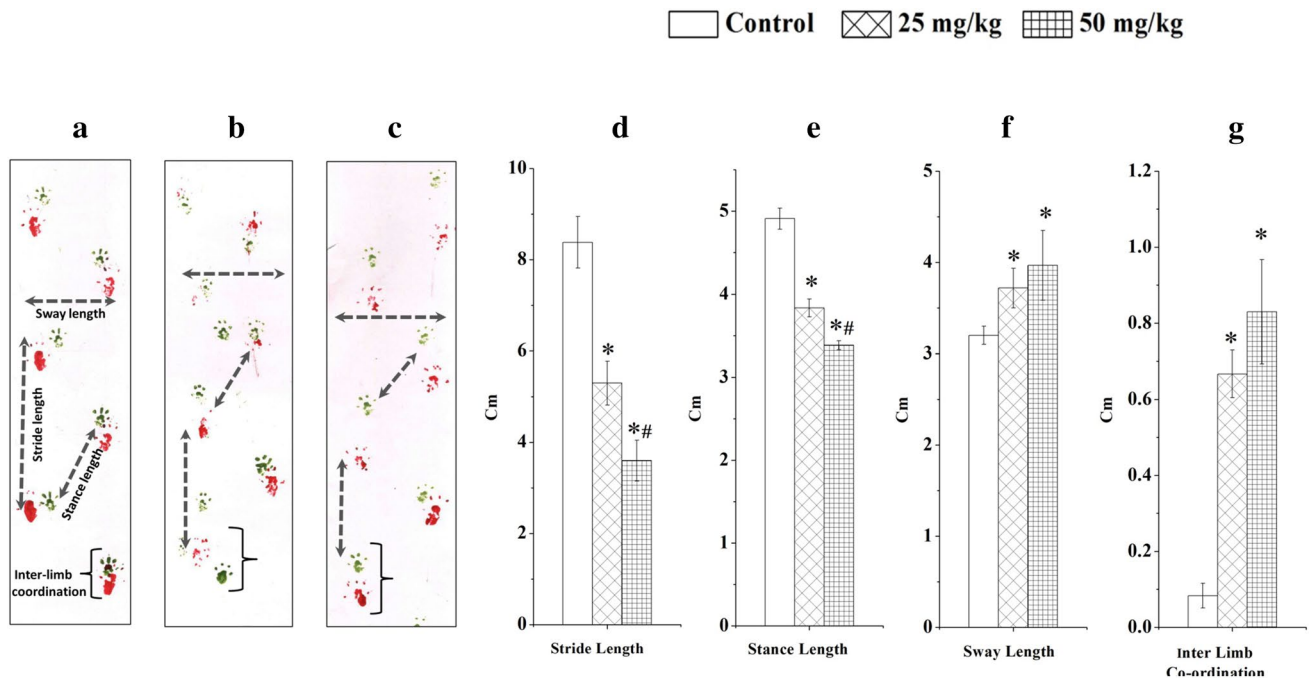

Fig. 2 Exposure to Fe_2O_3-NPs affects gait performance in mice. **a** Foot print of control, **b** 25 mg/kg and **c** 50 mg/kg treated mice. The analytical graph shows alteration in **d** stride length, **e** stance length, **f** sway length and **g** inter-limb coordination in mice after exposed with Fe_2O_3-NPs. Values are mean ± SD of five animals. *p < 0.05 compared to control animals; #p < 0.05 compared to 25 mg/kg treated animals (one-way ANOVA followed by Tukey's multiple comparison test)

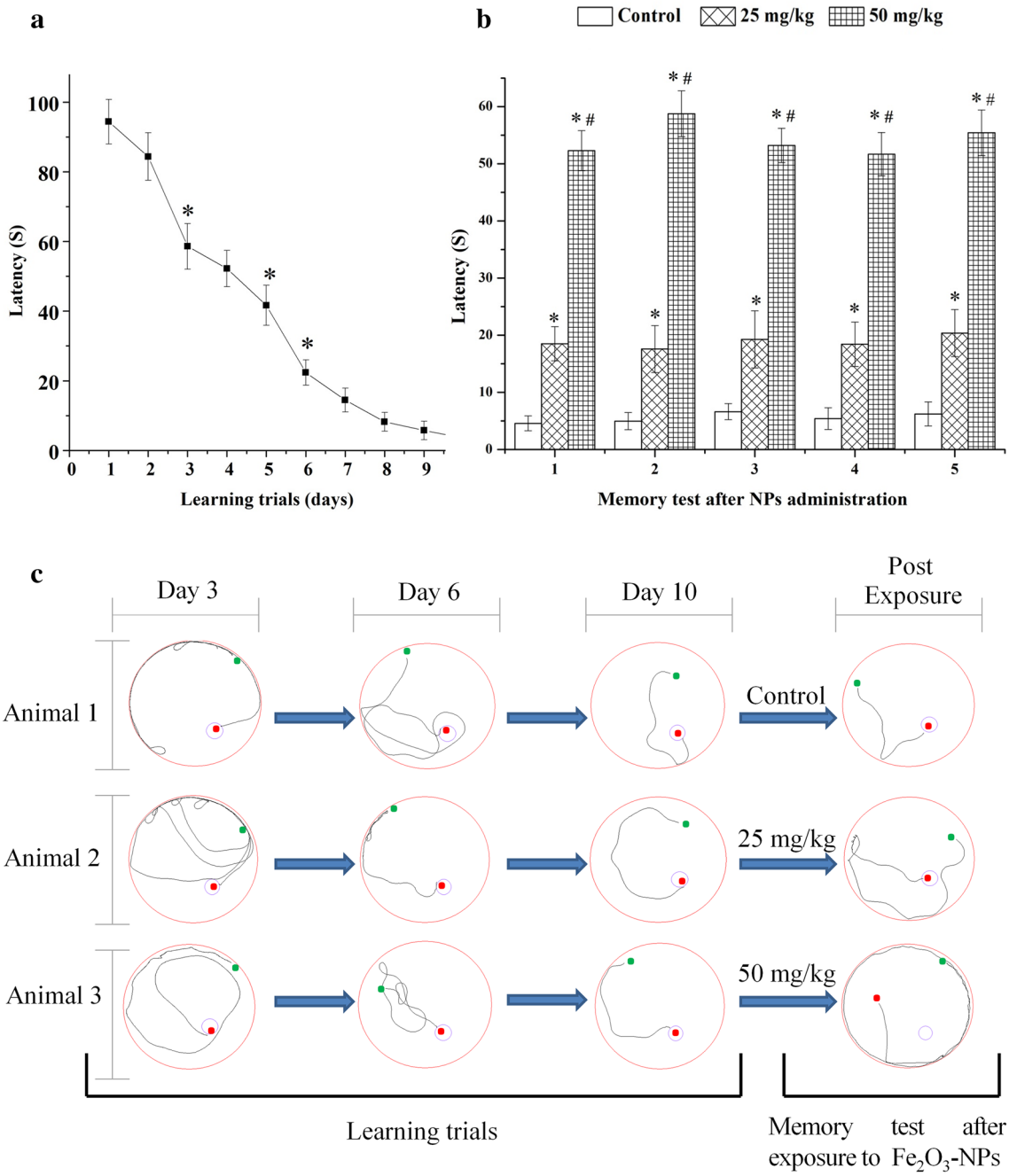

Fig. 3 Exposure to Fe_2O_3-NPs impairs learning and memory in mice. **a** Learning trails and **b** spatial memory test after Fe_2O_3-NPs exposure shows the latency of five animals for five individual test. Values are mean ± SD of five animals. *p < 0.05 compared to control animals; #p < 0.05 compared to 25 mg/kg treated animals (one-way ANOVA followed by Tukey's multiple comparison test). **c** Representative trajectory path image of control and test animals

Fe_2O_3-NPs Alters Electrolyte Concentrations and ATPase Activities

Electrolyte (Mg^{2+}, Na^+ and K^+) levels were significantly increased in serum and brain tissues of Fe_2O_3-NPs treated groups. Levels of Na^+ was significantly increased in the tissues of frontal cortex, hippocampus and was decreased in cerebellum of treated groups. K^+ was significantly increased in the tissues of frontal cortex and hippocampus. Cerebellum shows decreased level of K^+ in 25 mg/kg treated group and Mg^{2+} was significantly increased in all the brain regions of treated groups (Table 1). Biochemical analysis shows that the exposure to Fe_2O_3-NPs

Table 1 Ion estimation in the serum and brain regions of control and treated animals

Ion	Serum and brain regions	Control	25 mg/kg	50 mg/kg
Fe^{2+}	Serum	22.2 ± 1.3	33.1 ± 2.2*	38.5 ± 1.4*#
	Frontal cortex	10.9 ± 0.8	13.9 ± 0.7*	17.6 ± 1.2*#
	Hippocampus	14.8 ± 1.0	20.2 ± 0.5*	23.5 ± 0.6*#
	Cerebellum	19.3 ± 2.2	37.2 ± 4.3*	58.3 ± 3.6*#
	Serum	53.3 ± 2.9	85.3 ± 3.4*	118.2 ± 5.3*#
	Frontal cortex	12.7 ± 0.5	10.2 ± 0.6*	10.7 ± 0.7*
Mg^{2+}	Hippocampus	20.5 ± 1.3	36.8 ± 2.1*	54.18 ± 2.9*#
	Cerebellum	41.5 ± 2.4	52.6 ± 3.9*	70.68 ± 3.4*#
	Serum	279.4 ± 34.5	2035.7 ± 53.5*	2562.8 ± 62.8*#
	Frontal cortex	192.3 ± 11.2	277.2 ± 21.9*	1995.4 ± 45.8*#
Na^{+}	Hippocampus	431.4 ± 23.4	274.8 ± 13.9*	1136.5 ± 53.9*#
	Cerebellum	489.2 ± 29.8	221.9 ± 21.3*	320.4 ± 17.3*#
	Serum	1420.7 ± 32.5	2934.3 ± 64.3*	3710.8 ± 43.5*#
	Frontal cortex	70.7 ± 10.4	28.8 ± 5.6*	44.3 ± 7.6*#
K^{+}	Hippocampus	561.6 ± 34.7	1925.7 ± 67.5*	2898.0 ± 46.7*#
	Cerebellum	2020.4 ± 42.4	1165.9 ± 32.4*	1941.4 ± 22.5*#

Unit: µg/dl serum; µg/g wet tissue. Values are mean ± SD of five animals in each group

*p < 0.05 significantly different from control

#p < 0.05 significantly different from 25 mg/kg Fe_2O_3-NPs treated mice (One-way ANOVA followed by Tukey's multiple comparison test)

significantly reduces the activity of Mg^{2+} and N^{+}/K^{+} ATPases in all the subjected brain regions (Table 2).

Fe_2O_3-NPs Causes Lipid Peroxidation and Axonal Demyelination

A significant increase in MDA levels in the frontal cortex, hippocampus and cerebellum were noticed in the treated groups (Fig. 5a). The cross-sections of axons were observed under TEM. Control neuronal axons with normal myelination in all the brain regions, whereas, Fe_2O_3-NPs treated animals were observed with demyelinated axons (Fig. 5b).

Effect of Fe_2O_3-NPs on Vesicular Exocytosis

Increased serum Ca^{2+} was observed (Fig. 6a) in NPs treated group. Vesicular exocytosis was indirectly assessed by analysing the level of $[Ca^{2+}]_i$ and expression of GAP43. A significant increase of $[Ca^{2+}]_i$ was found in the Fe_2O_3-NPs treated brain regions (Fig. 6b, c). Western blotting and IHC reveals the reduction in the expression level of GAP43 (Fig. 6d, e). Frontal cortex and hippocampus of treated group show dose dependant reduction in Ca^{2+}ATPase activity, whereas cerebellum of 50 mg/kg treated group shows decrease in the Ca^{2+}ATPase activity compared to control, however statistically insignificant (Table 3).

Fe_2O_3-NPs Alters Monoamine Metabolism

Semi-quantitative RT-PCR results show the gene expression pattern of *Th*, *MAO-A* and *B*. The expression of *Th* was increased in frontal cortex and hippocampus and there was no much change observed in cerebellum (Fig. 7a). Gene expression of *MAO-A* was increased in all the subjected brain regions of treated animals. *MAO-B* was increased in frontal cortex and hippocampus, whereas cerebellum shows almost equal expression in treated animals compared to control. Biochemical activity of MAO-A was significantly increased in hippocampus (Fig. 7b). However, MAO-B activity was found to be increased in the NPs treated brain regions (Fig. 7c). Quantification of monoamines by HPLC reveals decreased DA and EP levels in the brain regions of Fe_2O_3-NPs treated groups. But, NE level was found to be increased in all the brain regions (Fig. 7d–f).

GFAP Expression

Western blotting and IHC results shows increased GFAP levels in Fe_2O_3-NPs treated groups compared to control (Fig. 8).

Discussion

In the past decades, neurotoxicity of Fe_2O_3-NPs has been studied extensively, but with less emphasize on animal behaviour. The present study is intended to give a collective

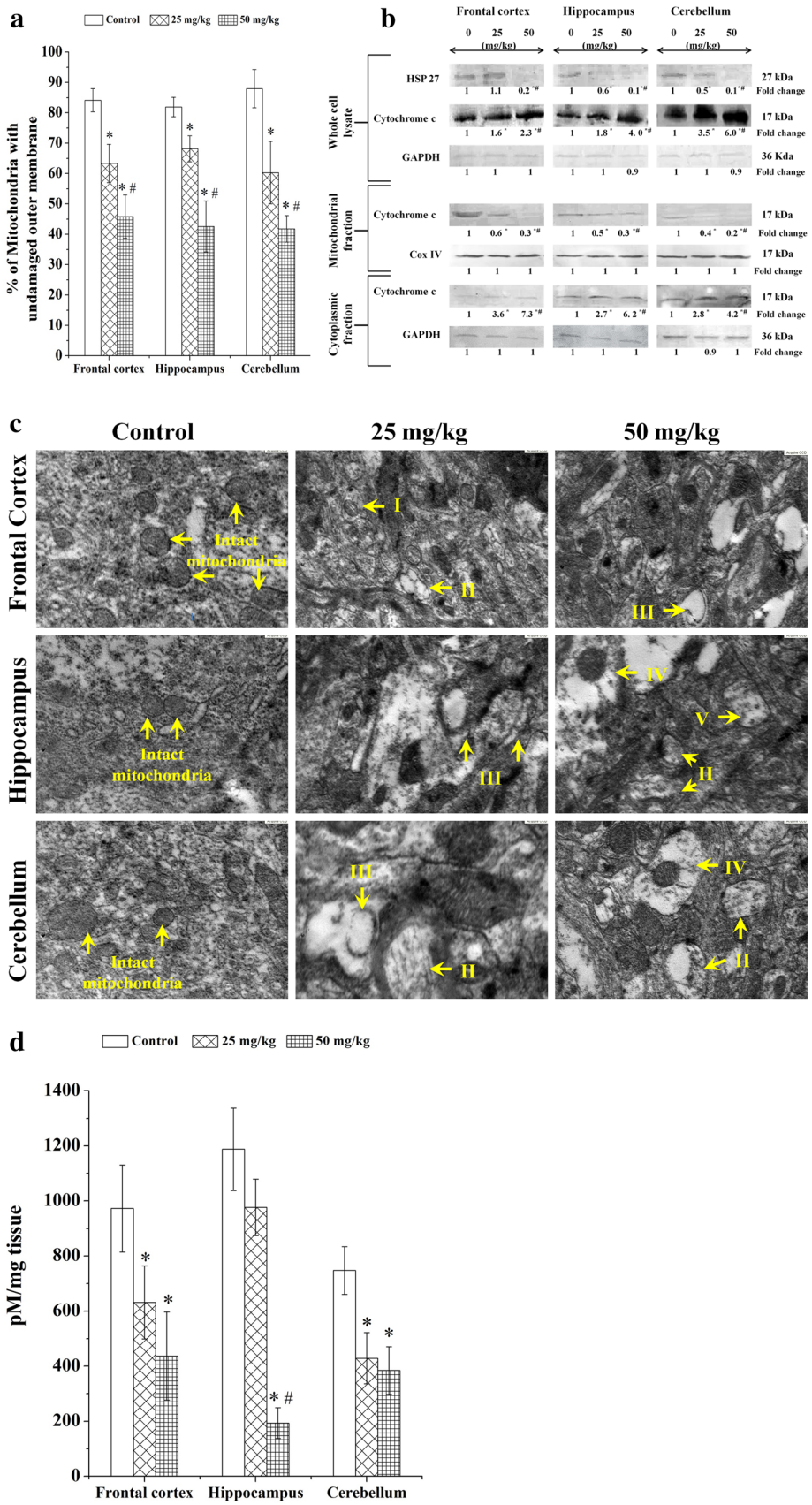

Fig. 4 Exposure to Fe_2O_3-NPs damages mitochondria and depletes energy in mice neurons. **a** % of mitochondria with undamaged outer membrane. **b** Immunoblotting analysis of HSP27 and cytochrome c from whole cell lysate of control and treated brain regions. Mitochondrial and cytoplasmic fractions were probed to check the levels of cytochrome c. **c** Ultrastructural changes in the neurons (500 nm scale). Control brain regions show intact mitochondria. Treated brain regions shows damaged mitochondria—vacuoles inside mitochondria (I), cristolysis (II), mitochondrial membrane damages (III), vacuoles around mitochondria (IV) and swollen mitochondria (V). **d** Luciferase assay shows the level of ATP in the brain regions of control and treated animals. Values are mean ± SD of five animals in each group. *p < 0.05 significantly different from control; #p < 0.05 significantly different from 25 mg/kg Fe_2O_3-NPs treated mice (one-way ANOVA followed by Tukey's multiple comparison test)

Table 2 Alteration in the activity of Mg^{2+} ATPase and N^+/K^+ ATPase in control and Fe_2O_3 NPs treated mice

ATPase	Brain regions	Control	25 mg/kg	50 mg/kg
Mg^{2+} ATPase	Frontal cortex	33.6 ± 3.0	26.5 ± 2.7*	18.3 ± 3.5*#
	Hippocampus	38.4 ± 2.4	26.4 ± 2.9*	18.9 ± 3.1*#
	Cerebellum	22.4 ± 1.2	19.2 ± 2.1	16.0 ± 1.8*
Na^+/K^+ ATPase	Frontal cortex	33.96 ± 2.0	26.5 ± 2.0*	20.2 ± 1.9*#
	Hippocampus	27.87 ± 2.8	26.6 ± 2.8	20.5 ± 2.5*#
	Cerebellum	27.17 ± 3.3	24.0 ± 2.9	17.8 ± 1.7*#

Unit: μM of Pi liberated/min/mg protein. Values are mean ± SD of five animals in each group

*p < 0.05 significantly different from control

#p < 0.05 significantly different from 25 mg/kg Fe_2O_3-NPs treated mice (One-way ANOVA followed by Tukey's multiple comparison test)

view on the impacts of Fe_2O_3-NPs on neurobehavior focusing more on monoamines. Mitochondria are the organelle of energy metabolism, where optimum iron level and cytochrome c plays a vital role in electron transport chain. But, in the case of iron accumulation, the excessive iron undergoes Fenton's reaction and generates reactive oxygen species to which mitochondria are more vulnerable right from the membranes to its internal structures [37]. HSP27 is a crucial stress response protein that protects cytochrome c intact within the mitochondrial inner membrane [38]. Downregulation of HSP27 in the brain regions of Fe_2O_3-NPs treated groups suggests the release of cytochrome c from the mitochondria. Reduction in the percent of mitochondria with intact membranes suggests the release of cytochrome c from mitochondria to cytoplasm. The cascade of these events eventually constitutes the energy depletion in the brain regions of treated animals. Mitochondrial damage and metabolic dysfunction seems to be associated with cognitive deficits [39].

Further, neuronal excitability consumes the maximum ATP generated during oxidative phosphorylation [40]. More than half of the total ATP generated in the brain at resting state is consumed by Na^+/K^+ ATPase to maintain proper transmembrane ionic gradients [41] and ion homeostasis for neuronal communication [42]. Significant decrease in the activity of Na^+/K^+ ATPase and tissue accumulation of Na^+ and K^+ suggest the inadequacy to maintain the tissue ion homeostasis in the Fe_2O_3-NPs treated animals. In addition, increased level of Mg^{2+} has shown to cause neurodegeneration by supressing neuronal excitability [43]. Since ATP is the substrate for ATPase, energy (ATP) depletion in the treated animals explains the decreased Mg^{2+}, Na^+/K^+ ATPase activity resulting in disturbed ion homeostasis. Expenditure of cellular energy is proportional to the strength of action potential and continuous firing [44]. Oral exposure to Fe_2O_3-NPs has been shown to inhibit the activity of Ca^{2+}, Na^+/K^+ and Mg^{2+}ATPase in rat brain [17].

Neuronal electric conductivity majorly depends on the levels of $[Ca^{2+}]_i$ and electrolytes [45]. Increased cytoplasmic Ca^{2+} elicits the fusion of synaptic vesicles with the

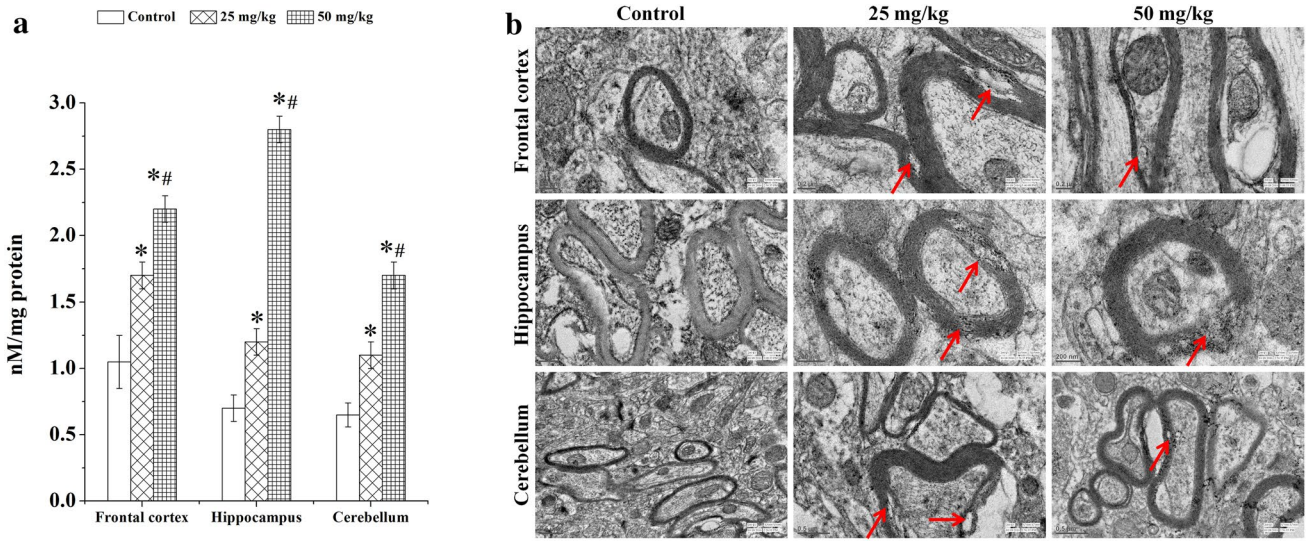

Fig. 5 Exposure to Fe_2O_3-NPs induces lipid peroxidation and axonal demyelination in mice neurons. **a** LPO and **b** TEM analysis shows normal myelination in the control and increased degree of demyelination in the treated brain regions (frontal cortex and hippocampus 200 nm scale; cerebellum 500 nm scale). The arrow indicates the sites of demyelination due to Fe_2O_3-NPs intoxication. Values are mean ± SD of five animals in each group. *p < 0.05 significantly different from control; #p < 0.05 significantly different from 25 mg/kg Fe_2O_3-NPs treated mice (one-way ANOVA followed by Tukey's multiple comparison test)

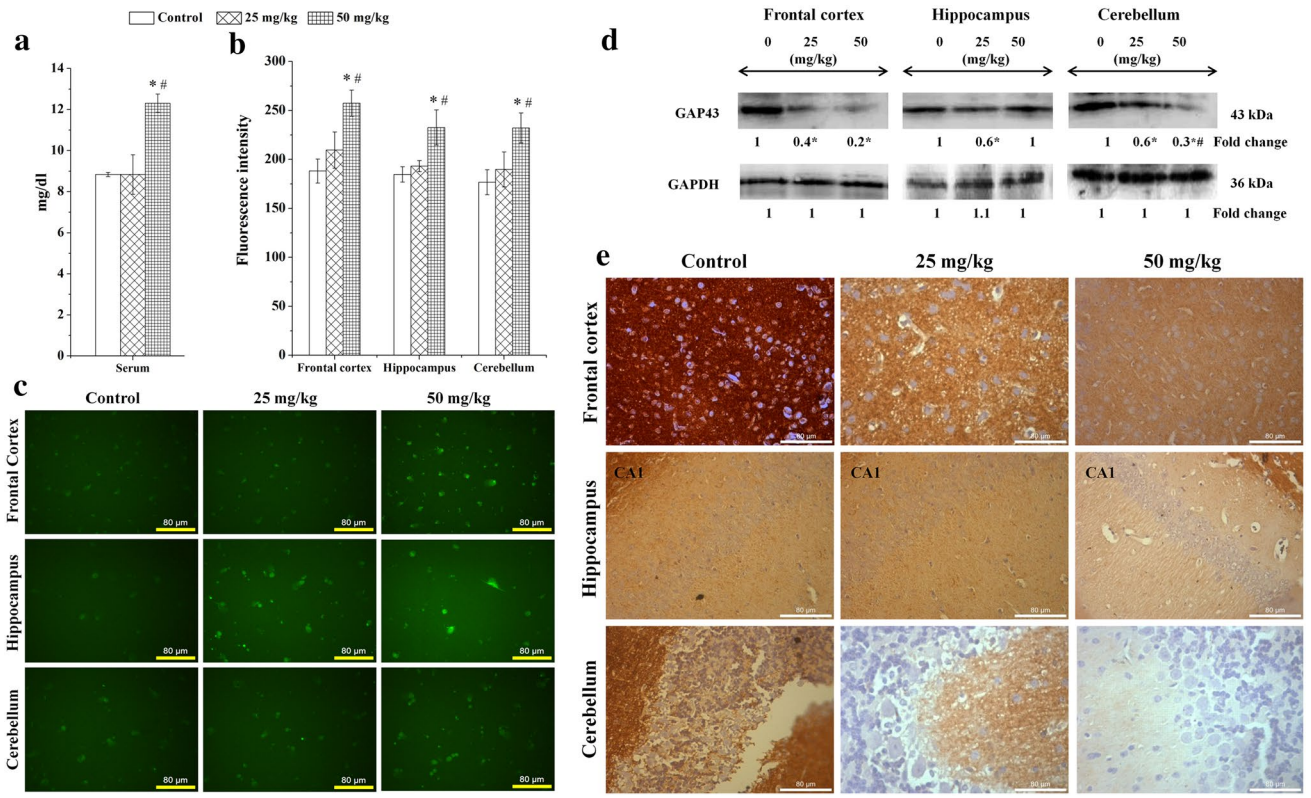

Fig. 6 Exposure to Fe_2O_3-NPs causes defects in vesicular exocytosis in mice brain. **a** Serum calcium level and **b** $[Ca^{2+}]_i$ in brain regions (Frontal cortex, hippocampus and cerebellum) of control and treated groups. **c** Fluorescence imaging of $[Ca^{2+}]_i$ in the primary cells isolated from the brain regions of control and test animals (80 µm scale). **d** Expression level of GAP43 in control and Fe_2O_3-NPs treated brain regions western blotting and **e** immunohistochemistry. Values are mean ± SD of five animals in each group. *p < 0.05 significantly different from control; #p < 0.05 significantly different from 25 mg/kg Fe_2O_3-NPs treated mice (one-way ANOVA followed by Tukey's multiple comparison test)

Table 3 Alteration in the activity of Ca^{2+} ATPase in control and Fe_2O_3-NPs treated mice

ATPase	Brain regions	Control	25 mg/kg	50 mg/kg
Ca^{2+} ATPase	Frontal cortex	32.1 ± 2.5	24.7 ± 2.4*	17.3 ± 2.8*#
	Hippocampus	36.8 ± 2.1	23.2 ± 2.7*	17.9 ± 2.7*#
	Cerebellum	19.9 ± 1.9	17.1 ± 2.1	15.5 ± 1.4*

Unit: µM of Pi liberated/min/mg protein. Values are mean ± SD of five animals in each group

*p < 0.05 significantly different from control

#p < 0.05 significantly different from 25 mg/kg Fe_2O_3-NPs treated mice (One way ANOVA followed by Tukey's multiple comparison test)

plasma membrane [46]. Alteration in Ca^{2+} homeostasis leads to impaired vesicular exocytosis and affects neurotransmitter release [47]. Thus the imbalance in Ca^{2+} levels and Ca^{2+}ATPase activity by Fe_2O_3-NPs can disturb the ion homeostasis in brain and affect the normal physiology. Excessive $[Ca^{2+}]_i$ [48] and released cytochrome c [38] were involved in neuronal apoptosis.

During the process of interneuronal communication, $[Ca^{2+}]_i$ interacts with GAP43 which facilitates the synoptic vesicular exocytosis [49]. Though the treated group experiences increased $[Ca^{2+}]_i$, down regulation of GAP43 suggest the impaired vesicular exocytosis. Loss of synaptic

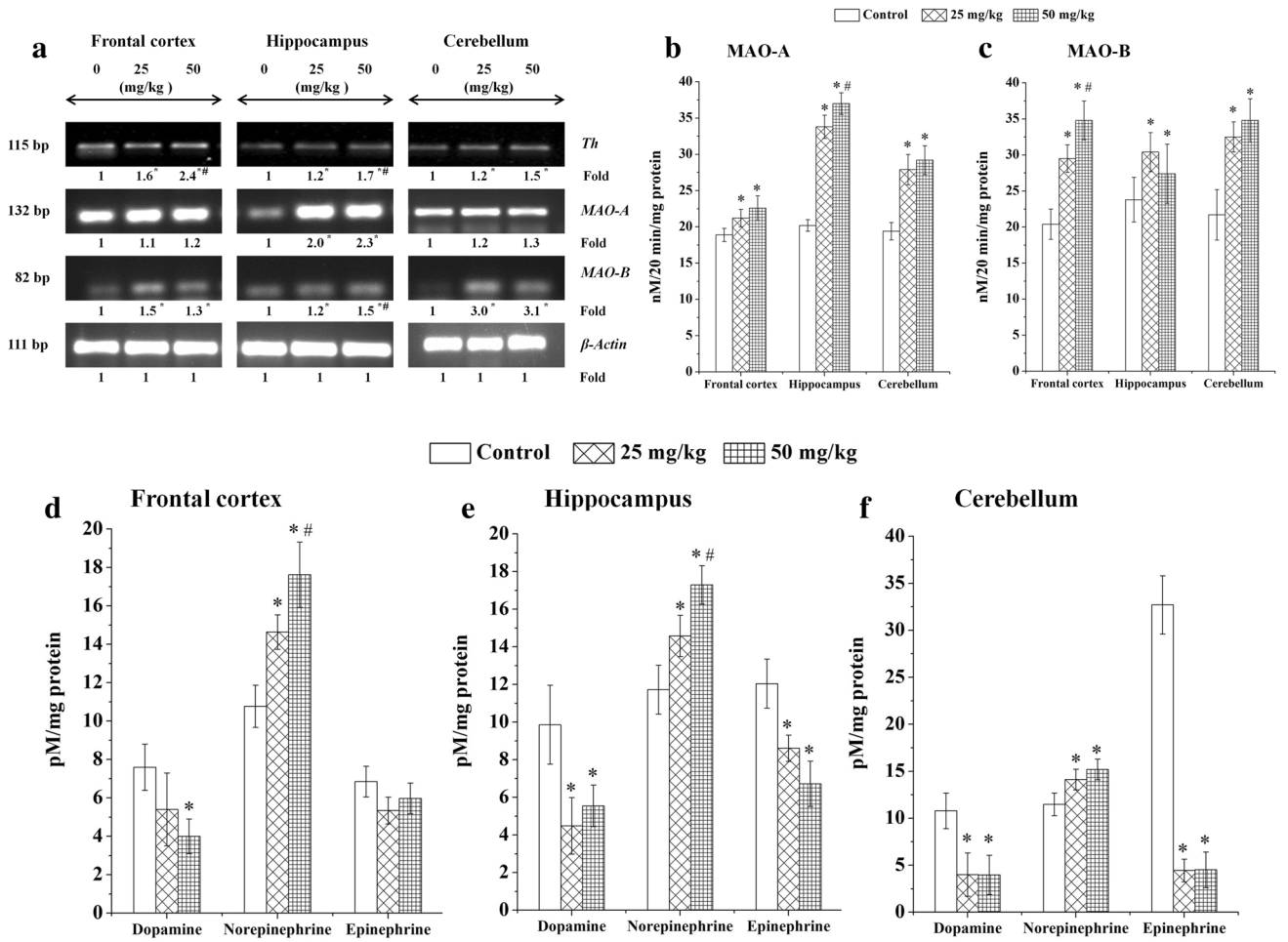

Fig. 7 Exposure to Fe_2O_3-NPs alters monoamine metabolism in mice. **a** Semi-quantitative RT-PCR expression of *Th, MAO-A* and *B* in control and Fe_2O_3-NPs treated brain regions. Biochemical activity of **b** MAO-A, **c** MAO-B. HPLC analysis of DA, NE and EP in **d** frontal cortex, **e** hippocampus and **f** cerebellum of control and Fe_2O_3-NPs treated groups. Values are mean ± SD of five animals in each group. *p < 0.05 significantly different from control, #p < 0.05, significantly different from 25 mg/kg Fe_2O_3-NPs treated mice (one-way ANOVA followed by Tukey's multiple comparison test)

connectivity has been shown in GAP43$^{-/-}$ mice [50]. Myelin sheath around the axons protects the neuronal electric conductivity intact [51]. The axonal demyelination in the brain regions suggest the loss of axonal insulation and thus the electric conductivity leakage which might lead to defective intra neuronal impulse transfer. The lipid peroxidation of brain tissues by Fe_2O_3-NPs has been correlated to demyelination [52] that attribute to impaired vesicular exocytosis which accentuates defective neuronal communication. Further, axonal demyelination seems to decline conduction velocity of action potential [53] and irreversible sensorimotor and cognitive deficits [54]. Figure 9 shows the schematic representation of Fe_2O_3-NPs induced neuronal defects.

Fe ion plays a remarkable role in neuronal metabolism, as they involve in synthesis and packaging of neurotransmitters [55]. Iron is a cofactor for Th, a key rate limiting enzyme responsible for the synthesis of monoamines [56]. Thus, increased Fe ion in brain regions due to Fe_2O_3-NPs should have increased all the monoamine levels hypothetically. On the contrary, inconsistent levels of monoamines were observed in our study insinuating the involvement of MAOs. Mice treated with 21 nm and 280 nm Fe_2O_3-NPs show change in the levels of NE in hippocampus [12]. Monoamine metabolism has significant impact on neuronal communication [57] and degeneration [58]. Normal level of monoamines in frontal cortex, hippocampus and cerebellum are essential for learning and memory [59]. Iron overload in rat has been reported to alter the hippocampal monoamines level resulting in cognitive defect [60] and locomotor impairments [61]. Fe_2O_3-NPs alters monoamine metabolism which explains the impaired locomotor behaviour and memory observed in the current study.

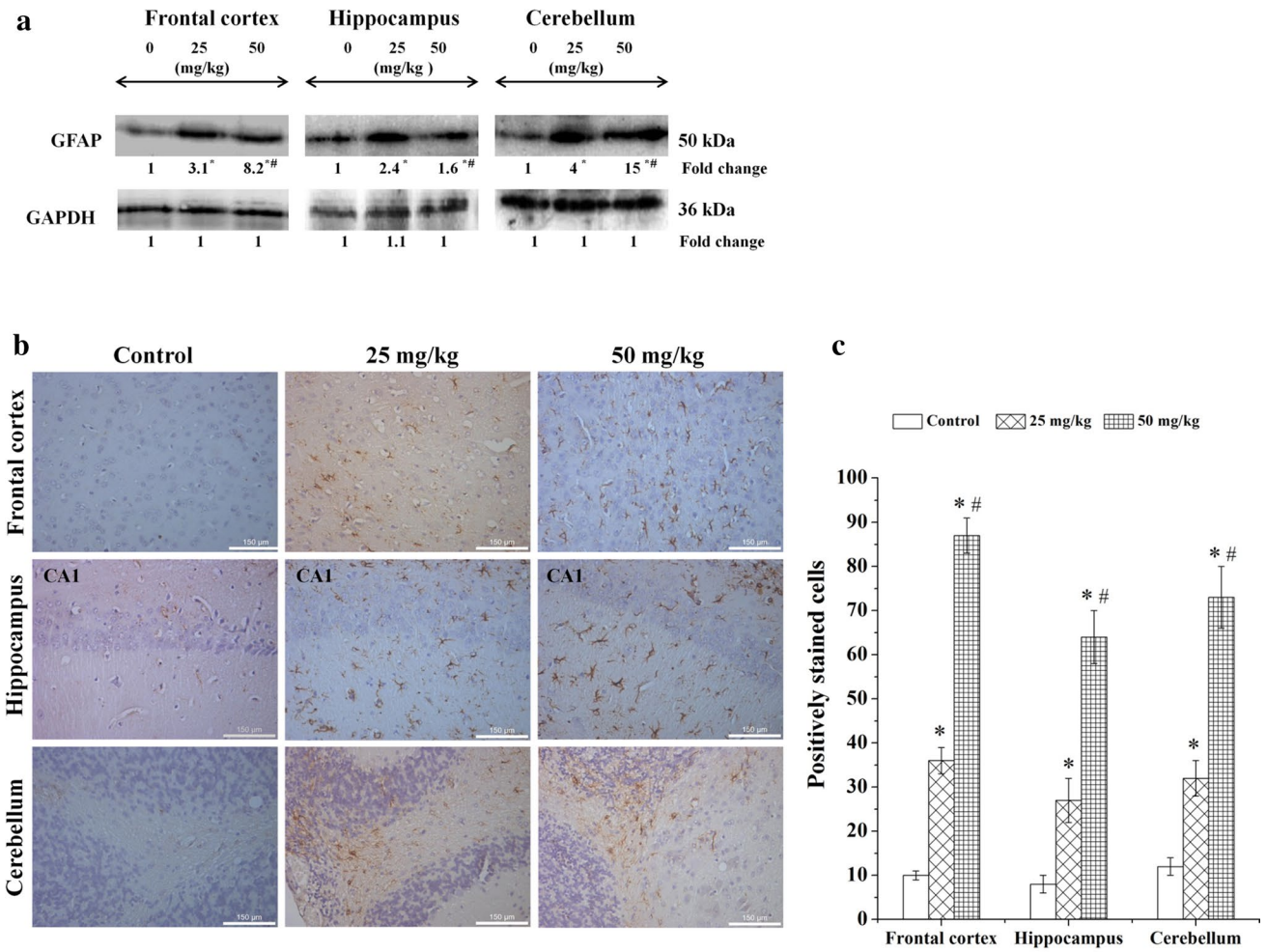

Fig. 8 Exposure to Fe_2O_3-NPs increases GFAP expression in brain regions. **a** Immunoblotting **b** Immunohistochemistry (150 μm scale) and **c** histogram shows positively stained cells of GFAP over expression. Values are mean ± SD of five animals in each group. *p < 0.05 significantly different from control; #p < 0.05 significantly different from 25 mg/kg Fe_2O_3-NPs treated mice (one-way ANOVA followed by Tukey's multiple comparison test)

Decreased levels of DA could be explained by the increased activity of MAO-B, because MAO-B has substrate affinity for DA [62]. Likewise, the quantity of NE is governed by the MAO-A [59]. Both MAO-A and B has less affinity for EP degradation [63]. The unaltered level of NE and EP is due to the insignificant expression level of *MAO-A* and less affinity of MAOs. Apart from the expression of *MAO-B*, it is also to be noted that NE has a negative feedback inhibition of *Th* [64]. Additionally, the expression level of *MAO-A* is unaltered in cerebellum, revealing that increased expression of *MAO-B* has no significant role in EP degradation [65]. *MAO-A* expression is associated with increased $[Ca^{2+}]_i$ in mice [66]. Th-deficiency syndrome is associated with most of the neurodegenerative diseases [67, 68]. Thus iron accumulation due to Fe_2O_3-NPs exposures alters catecholamine metabolism (Fig. 10).

GFAP is an astroglyosis marker expressed in response to CNS injuries [69]. An increased level of GFAP was observed in neurodegenerative disorders including stroke [70], multiple sclerosis [71], cerebral infarctions [72], subarachnoid haemorrhage [73] and traumatic brain injuries [74]. In addition,

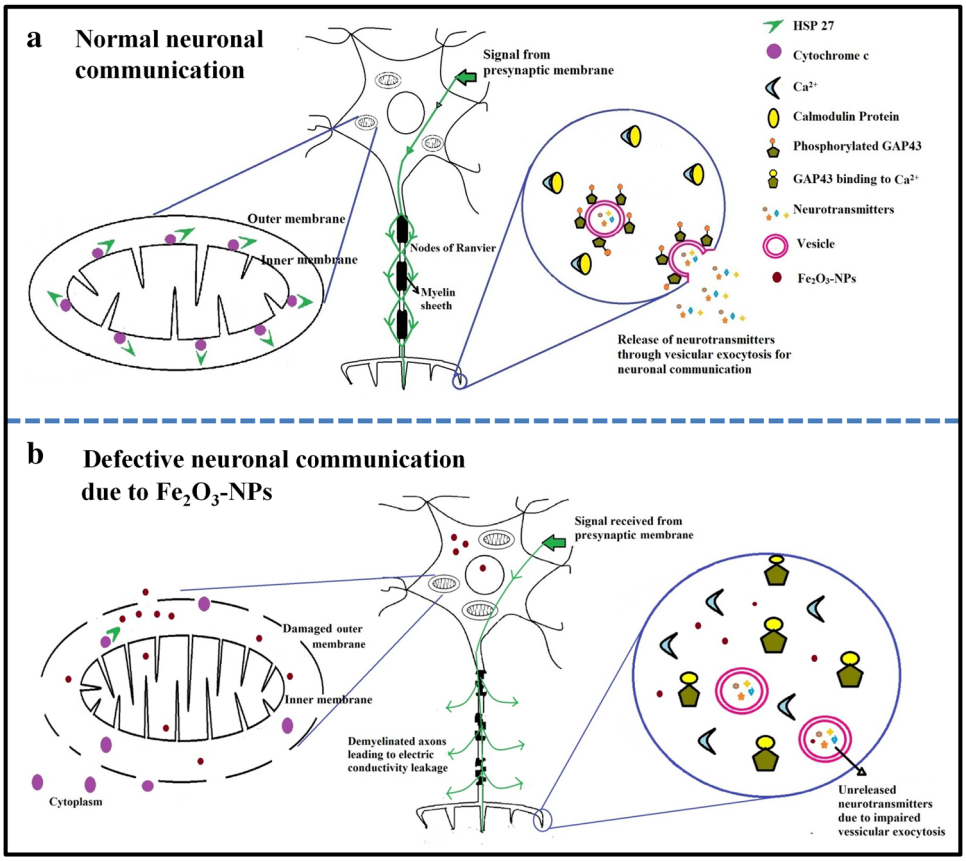

Fig. 9 Schematic representations of Fe_2O_3-NPs mediated neuronal defects. **a** Normal neuronal physiology with undamaged mitochondria. The cytochrome c resides in the mitochondrial inner membrane are protected by HSP27. The axons are properly insulated by spingolipids (spingomyelin) and thus ensure the proper intra neuronal impulse transfer from the cell body to the axonal terminals, jumping through the nodes of Ranvier. At axonal terminals, influx of Ca^{2+} occurs as a result of action potential, leading to the release of GAP43 from CAM and resulting in the phosphorylation of GAP43. Consequently, the vesicles consisting neurotransmitters are transported to the neuronal membrane by the process called vesicular exocytosis, with the aid of numerous other proteins. Finally neurotransmitters are released into synapsis for inter neuron communication. **b** Accumulation of iron due to Fe_2O_3-NPs in the brain regions results in mitochondrial damages. Reduction in HSP27 level leads to the release of cytochrome c from mitochondrial inner membrane to the cytoplasm via the damaged outer membrane, leading to energy depletion. The axons were demyelinated due to Fe_2O_3-NPs leading to impaired intra neuronal impulse transfer. The signals are not communicated through the nodes of Ranviers and they are lost at the sites of demyelination. Consequently, the axonal terminal receives poor signal. Though the influx of Ca^{2+} is high, the reduced GAP43 level results in defective vesicular exocytosis. All these events collectively suggest that Fe_2O_3-NPs intoxication affects neuronal signal transfer and communication

GFAP over expression is a hallmark for astrocytes activation in most of the neurodegenerative diseases including Alzheimer's disease [75] and Amyotrophic lateral sclerosis [76]. Thus, the elevated level of GFAP observed in this study reveals a possibility of brain injury with impaired communication in the test animals.

Conclusions

In conclusion, our study underlies that repeated ingestion of Fe_2O_3-NPs affects the factors associated with neuronal communication leading to neurobehavioural impairments in mice. However, detailed studies at inter- and intra

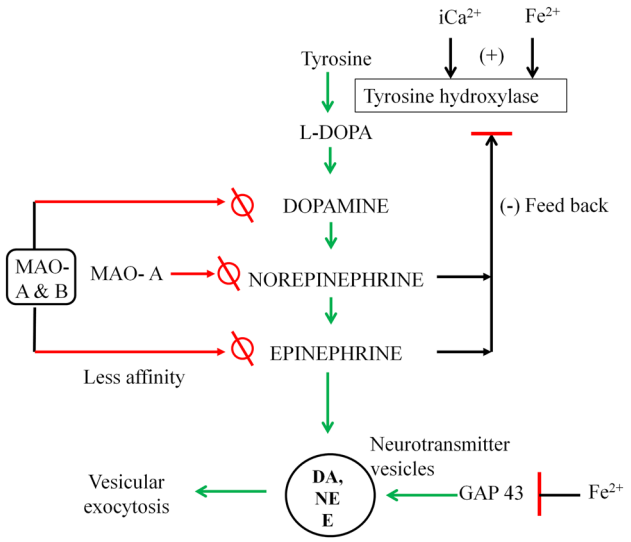

Fig. 10 Fe_2O_3-NPs alters monoamine metabolism. Tyrosine is converted to L-DOPA by tyrosine hydroxylase (Th). L-DOPA leads to the synthesis of dopamine (DA) followed by norepinephrine (NE) and epinephrine (EP). The synthesized neurotransmitters are packed into vesicles that are released into synapsis by vesicular exocytosis with the help of GAP43. MAO-A and B are the oxidases having substrate affinity for DA. MAO-A has affinity for NE. Both oxidases have lesser affinity for EP. EP and NE have negative feedback mechanism for the rate limiting activity of Th. Fe^{2+} and iCa^{2+} has positive correlation with the Th activity. Fe accumulation also hampers the level of GAP43

cellular levels are required to confirm the accurate changes in the physiology of neuronal communication mediated by Fe_2O_3-NPs. Further, other descrete brain regions including striatum and midbrain nuclei upon the exposure to Fe_2O_3-NPs is also warranted, since their functions are also important for the animal behavior.

Acknowledgements The authors would like to acknowledge Sophisticated Analytical Instrument Facility, All India Institute of Medical science (AIIMS), New Delhi, for the technical assistance in transmission electron microscopy. The authors are also grateful to Mr. Monojit Bhattacharjee, Bharathiar University, Coimbatore, for his assistance in HPLC analysis. Vijayprakash Manickam acknowledges the UGC-BSR fellowship (UGC-BSR-No.F.7-25/2007) funded by UGC-BSR, New Delhi, India. We also thank the UGC-SAP DRS II (F-3-30/2013), DST FIST (SR/FST/LSI-618/2014) and DST-SERB (EMR/2014/000600), New Delhi, India for their partial financial assistance.

Compliance with Ethical Standards

Conflict of interest The authors declare no conflict of interest.

Ethical Approval All procedures performed in this study involving animals were in accordance with the ethical standards of the institution or practice at which the studies were conducted.

References

1. Wu W, Wu Z, Yu T, Jiang C, Kim WS (2015) Recent progress on magnetic iron oxide nanoparticles: synthesis, surface functional strategies and biomedical applications. Sci Technol Adv Mater 16:e023501
2. Weinstein JS, Varallyay CG, Dosa E, Gahramanov S, Hamilton B, Rooney WD, Muldoon LL, Neuwelt EA (2010) Superparamagnetic iron oxide nanoparticles: diagnostic magnetic resonance imaging and potential therapeutic applications in neurooncology and central nervous system inflammatory pathologies, a review. J Cereb Blood Flow Metab 30:15–35
3. Hahn PSFDD, Lewis JM, Saini S, Elizondo G, Weissleder R, Fretz CJ, Ferrucci JT (1990) First clinical trial of a new superparamagnetic iron oxide for use as an oral gastrointestinal contrast agent in MR imaging. Radiology 175:695–700
4. Johnson WK, Stoupis C, Torres GM, Rosenberg EB, Ros PR (1996) Superparamagnetic iron oxide (SPIO) as an oral contrast agent in gastrointestinal (GI) magnetic resonance imaging (MRI): comparison with state-of-the-art computed tomography (CT). Magn Reson Imaging 14:43–49
5. Lodhia J, Mandarano G, Ferris NJ, Eu P, Cowell SF (2010) Development and use of iron oxide nanoparticles (Part 1): synthesis of iron oxide nanoparticles for MRI. Biomed Imaging Interv J 6:e12
6. Yang Y, Glenn AL, Raine A (2008) Brain abnormalities in antisocial individuals: implications for the law. Behav Sci Law 26:65–83
7. Sun C, Fang C, Stephen Z, Veiseh O, Hansen S, Lee D, Ellenbogen RG, Olson J, Zhang M (2008) Tumor-targeted drug delivery and MRI contrast enhancement by chlorotoxin-conjugated iron oxide nanoparticles. Nanomedicine 3:495–505
8. Manickam V, Dhakshinamoorthy V, Perumal E (2018) Iron oxide nanoparticles induces cell cycle-Dependent neuronal apoptosis in mice. J Mol Neurosci 64:352–362
9. Wang J, Zhoua G, Chena C, Yu H, Wang T, Mad Y, Jia G, Gao Y, Li B, Suna J, Li Y, Jiao F, Zhao Y, Chai Z (2007) Acute toxicity and bio distribution of different sized titanium dioxide particles in mice after oral administration. J Toxicol Lett 168:176–185
10. Winer JL, Liu CY, Apuzzo ML (2012) The use of nanoparticles as contrast media in neuroimaging: a statement on toxicity. World Neurosurg 78:709–711
11. Wu J, Ding T, Sun J (2013) Neurotoxic potential of iron oxide nanoparticles in the rat brain striatum and hippocampus. Neurotoxicology 34:243–253
12. Wang B, Feng W, Zhu M, Wang Y, Wang M, Gu Y, Ouyang H, Wang H, Li M, Zhao Y, Chai Z, Wang H (2009) Neurotoxicity of low-dose repeatedly intranasal instillation of nano- and submicron-sized ferric oxide particles in mice. J Nanopart Res 11:41–53
13. Yarjanli Z, Kamran G, Abolghasem E, Soheila R, Ali Z (2017) Iron oxide nanoparticles may damage to the neural tissue through iron accumulation, oxidative stress, and protein aggregation. BMC Neurosci 18:51–67
14. De Lima MN, Polydoro M, Laranja DC, Bonatto F, Bromberg E, Moreira JC, Dal-Pizzol F, Schröder N (2005) Recognition memory impairment and brain oxidative stress induced by postnatal iron administration. Eur J Neurosci 21:2521–2528
15. Fredriksson A, Schroder N, Eriksson P, Izquierdo I, Archer T (2000) Maze learning and motor activity deficits in adult mice induced by iron exposure during a critical postnatal period. Brain Res Dev 119:65–74
16. Dhakshinamoorthy V, Manickam V, Perumal E (2017) Neurobehavioural toxicity of iron oxide nanoparticles in mice. Neurotox Res 32:187–203
17. Kumari M, Rajak S, Singh SP, Kumari SL, Kumar PU, Murty USN, Mahboob M, Grover P, Rahman MF (2012) Repeated oral

dose toxicity of iron oxide nanoparticles: biochemical and histopathological alterations in different tissues of rats. Nanosci Nanotechnol 12:2149–2159
18. Libersat F, Pflueger HJ (2004) Monoamines and the orchestration of behavior. Bioscience 54:17–25
19. Tzschentke TM (2001) Pharmacology and behavioral pharmacology of the mesocortical dopamine system. Prog Neurobiol 6:241–320
20. Michelotti GA, Price DT, Schwinn DA (2000) Alpha 1-adrenergic receptor regulation: basic science and clinical implications. Pharmacol Ther 88:281–309
21. Shetty PK, Galeffi F, Turner DA (2012) Cellular links between neuronal activity and energy homeostasis. Front Pharmacol 3:1–14
22. Estelrich J, María JSM, Maria AB (2015) Nanoparticles in magnetic resonance imaging: from simple to dual contrast agents. Int J Nanomed 10:1727–1741
23. Sundarraj K, Raghunath A, Panneerselvam L, Perumal E (2017) Iron oxide nanoparticles modulate heat shock proteins and organ specific markers in mice male accessory organs. Toxicol Appl Pharmacol 317:12–24
24. Paul V, Ekambaram P, Jayakumar AR (1998) Effects of sodium fluoride on locomotor behaviour and a few biochemical parameters in rats. Environ Toxicol Pharmacol 6:187–191
25. Ekambaram P, Paul V (2003) Effect of vitamin D on chronic behavioral and dental toxicities on sodium fluoride in rats. Fluoride 36(3):189–197
26. Dharmalingam P, Kulasekaran G, Ganapasam S (2013) Fisetin enhances behavioral performances and attenuates reactive gliosis and inflammation during aluminum chloride-induced neurotoxicity. NeuroMol Med 15:192–208
27. Wenk GL (2004) Assessment of spatial memory using the radial armmaze and Morris water maze. Curr Protoc Neurosci 26:8–15
28. Hjertén S, Pan H (1983) Purification and characterization of two forms of a low-affinity Ca2+-ATPase from erythrocyte membranes. Biochim et Biophys Acta 728:281–288
29. Ohnishi T, Suzuki T, Suzuki Y, Ozawa KA (1982) Comparative study of plasma membrane Mg2+-ATPase activities in normal, regenerating and malignant cells. Biochim Biophys Acta 684:67–74
30. Bonting SL, Caravaggio LL, Hawkins NM (1963) Studies on sodium-potassium-activated adenosine triphosphatase. VI. Its role in cation transport in the lens of cat, calf and rabbit. Arch Biochem Biophys 101:47–55
31. Devasagayam TP, Tarachand U (1987) Decreased lipid peroxidation in rat kidney during gestation. Biochem Biophys Res Commun 145:134–138
32. Kim JJ, Shih JC, Chen K, Chen LU, Bao S, Marten S, Anagnostaras SG, Fanselow MS, Maeyer ED, Seif I, Thompson RF (1997) Selective enhancement of emotional, but not motor, learning in monoamine oxidase A-deficient mice. Proc Natl Acad Sci USA 94:5929–5933
33. Chen K, Cases O, Rebrin I, Wu W, Gallaher TK, Seif I, Shih JC (2006) Forebrain-specific expression of monoamine oxidase a reduces neurotransmitter levels, restores the brain structure, and rescues aggressive behavior in monoamine oxidase a-deficient mice. J Biol Chem 282:115–123
34. Sheng L, Ze Y, Wang L, Yu X, Hong J, Zhao X, Ze X, Liu D, Xu B, Zhu Y, Long Y, Lin A, Zhang C, Zhao Y, Hong F (2015) Mechanisms of TiO2 nanoparticle-induced neuronal apoptosis in rat primary cultured hippocampal neurons. J Biomed Mater Res 103:1141–1149
35. Yang J, Liu Q, Wu S, Xi Q, Cai Y (2013) Effects of lanthanum chloride on glutamate level, intracellular calcium concentration and caspases expression in the rat hippocampus. Biometals 26:43–59
36. Yu JF, Kong LD, Chen Y (2002) Antidepressant activity of aqueous extracts of Curcuma longa in mice. J Ethnopharmacol 83:161–165
37. Guo C, Sun L, Chen X, Zhang D (2003) Oxidative stress, mitochondrial damage and neurodegenerative diseases. Neural Regen Res 8:2003–2014
38. Havasi A, Li Z, Wang Z, Martin JL, Botla V, Ruchalski K, Schwartz JH, Borkan SC (2008) Hsp27 inhibits Bax activation and apoptosis via a phosphatidylinositol 3-kinase-dependent mechanism. J Biol Chem 283:12305–12313
39. Lifshitz J, Kelley BJ, Povlishock JT (2007) Perisomatic thalamic axotomy after diffuse traumatic brain injury is associated with atrophy rather than cell death. J Neuropathol Exp Neurol 66:218–229
40. Magistretti PJ, Allaman IA (2015) Cellular perspective on brain energy metabolism and functional imaging. Neuron 86:883–901
41. Erecinska M, Silver IA (1989) ATP and brain function. J Cereb Blood Flow Metab 9:2–19
42. Yu SP (2013) Na^+, K^+-ATPase: the new face of old player in pathogenesis and apoptotic/hybrid cell death. Biochem Pharmacol 66:1601–1609
43. Dribben WH, Eisenman LN, Mennerick S (2010) Magnesium induces neuronal apoptosis by suppressing excitability. Cell Death Dis 1:1–9
44. Kadekaro M, Crane AM, Sokoloff L (1985) Differential effects of electrical stimulation of nerve on metabolic activity in spinal cord and dorsal root ganglion in the rat. Proc Natl Acad Sci USA 82:6010–6013
45. Oloche JJ, Obochi GO (2012) Sodium pump adaptability to tissue-specific regulation: a review. Asian J Biochem 10:180–189
46. Hay JC (2007) Calcium: a fundamental regulator of intracellular membrane fusion? EMBO 8:236–240
47. Thanawala MS, Regehr WG (2013) Presynaptic calcium influx controls neurotransmitter release in part by regulating the effective size of the readily releasable pool. J Neurosci 33:4625–4633
48. Xu B, Chen S, Luo Y, Chen Z, Liu L, Zhou H, Chen W, Shen T, Han X, Chen L, Huang S (2011) Calcium signaling is involved in cadmium-induced neuronal apoptosis via induction of reactive oxygen species and activation of MAPK/mTOR network. PLoS ONE 6:e19052
49. Tandon A, Bannykh S, Kowalchyk JA, Banerjee A, Martin TFJ, Balch WE (1998) Differential regulation of exocytosis by calcium and CAPS in semi-intact synaptosomes. Neuron 21:147–154
50. Latchney SE, Masiulis I, Zaccaria KJ, Lagace DC, Powell CM, Mc Casland JS, Eisch AJ (2014) Developmental and adult GAP-43 deficiency in mice dynamically alters hippocampal neurogenesis and mossy fiber volume. Dev Neurosci 36:44–63
51. Xing Y, Samuvel DJ, Stevens SM, Dubno JR, Schulte BA, Lang H (2012) Age-Related Changes of Myelin Basic Protein in Mouse and Human Auditory Nerve. PLoS ONE 7:1–15
52. Wang P, Xie K, Wang C, Bi J (2014) Oxidative stress induced by lipid peroxidation is related with inflammation of demyelination and neurodegeneration in multiple sclerosis. Eur Neurol 72:249–254
53. Coggan JS, Bittner S, Stiefel KM, Meuth SG, Prescott SA (2015) Physiological dynamics in demyelinating diseases: unraveling complex relationships through computer modeling. Int J Mol Sci 16:21215–21236
54. Shi HS, Luo YX, Yin X, Wu HH, Xue G, Geng XH (2015) Reconsolidation of a cocaine associated memory requires DNA methyltransferase activity in the basolateral amygdala. Sci Rep 5:e13327

55. Batra J, Sood A (2005) Iron deficiency anaemia: effect on cognitive development in children: a review. Indian J Clin Biochem 20:119–125
56. Bezem MT, Baumann A, Skjærven L, Meyer R, Kursula P, Martinez A, Flydal MI (2016) Stable preparations of tyrosine hydroxylase provide the solution structure of the full-length enzyme. Sci Rep 6:e30390
57. Lovinger DM (2008) Communication networks in the brain neurons, receptors, neurotransmitters and alcohol. Alcohol Res Health 31:196–214
58. Sasaki M, Shibata E, Tohyama K, Kudo K, Endoh J, Otsuka K, Sakai A (2008) Monoamine neurons in the human brain stem: anatomy, magnetic resonance imaging findings, and clinical implications. Neurorepor 19:1649–1654
59. Singh C, Bortolatob M, Bali N, Godard SC, Scottd AL, Chend K, Thompsona RF, Shiha JC (2012) Cognitive abnormalities and hippocampal alterations in monoamine oxidase A and B knockout mice. PNAS 110:12816–12821
60. Maaroufi K, Aissouni LH, Melonc C, Sakly M, Abdelmelek H, Poucet B, Save E (2014) Spatial learning, monoamines and oxidative stress in rats exposed to 900 MHz electromagnetic field in combination with iron overload. Behav Brain Res 258:80–89
61. Barbelivien A, Nyman L, Haapalinna A, Sirviö J (2001) Inhibition of MAO-A activity enhances behavioural activity of rats assessed using water maze and open arena tasks. Pharmacol Toxicol 88:304–312
62. Shih JC, Chen K, Ridd MJ (1999) Monoamine oxidase: from genes to behavior. Annu Rev Neurosci 22:197–217
63. Eisenhofer G, Finberg JP (1994) Different metabolism of norepinephrine and epinephrine by catechol-O-methyltransferase and monoamine oxidase in rats. J Pharmacol Exp Ther 268:1242–1251
64. Daubner SC, Le T, Wang S (2011) Tyrosine hydroxylase and regulation of dopamine synthesis. Arch Biochem Biophys 508:1–12
65. Bortolato M, Shih JC (2011) Behavioral outcomes of monoamine oxidase deficiency: preclinical and clinical evidence. Int Rev Neurobiol 100:13–42
66. Lee HY, Lee GH, Marahatta A, Lin SM, Lee MR, Jang KY, Kim KM, Lee HJ, Lee JW, Bagalkot TR, Chung YC, Lee YC, Kim HR, Chae HJ (2013) The protective role of Bax Inhibitor-1 against chronic mild stress through the inhibition of monoamine oxidase A. Sci Rep 3:e3398
67. Tabrez S, Jabir NR, Shakil S, Greig NH, Alam Q, Abuzenadah AM, Damanhouri GA, Kamal MA (2012) A synopsis on the role of tyrosine hydroxylase in Parkinson's disease. CNS Neurol Disord: Drug Targets 11:395–409
68. Nakashima A (2012) Proteasomal degradation of tyrosine hydroxylase and neurodegeneration. J Neurochem 120:199–201
69. Rosengren L, Wikkelso C, Hagberg L (1994) A sensitive ELISA for glial fibrillary acidic protein-application in CSF of adults. J Neurosci Methods 51:197–213
70. Herrmann MI, Vos P, Wunderlich MT, de Bruijn CH, Lamers KJ (2000) Release of glial tissue-specific proteins after acute stroke: a comparative analysis of serum concentrations of protein S-100B and glial fibrillary acidic protein. Stroke 31:2670–2677
71. Rosengren LE, Lycke J (1995) Andersen. Glial fibrillary acidic protein in CSF of multiple sclerosis patients: relation to neurological deficit. J Neurol Sci 133:61–65
72. Nylén K, Karlsson JE, Blomstrand C, Tarkowski A, Trysberg E, Rosengren LE (2002) Cerebrospinal fluid neurofilament and glial fibrillary acidic protein in patients with cerebral vasculitis. J Neurosci Res 67:844–851
73. Petzold A, Keir G, Kay A, Kerr M, Thompson EJ (2006) Axonal damage and outcome in subarachnoid haemorrhage. J NeurolNeurosurg Psychiatry 77:753–759
74. Vos PE, Jacobs B, Andriessen TM, Lamers KJ, Borm GF, Beems T (2010) GFAP and S100B are biomarkers of traumatic brain injury: an observational cohort study. Neurology 75:1786–1793
75. Brahmachari S, Fung YK, Pahan K (2006) Induction of glial fibrillary acidic protein expression in astrocytes by nitric oxide. The Journal of Neuroscience 26:4930–4939
76. Vargas MR, Johnson JA (2010) Astrogliosis in amyotrophic lateral sclerosis: role and therapeutic potential of astrocytes. Neurotherapeautics 7:471–481